



RESEARCH ARTICLE

Open Access



# Impacts of land reclamation projects on hydrodynamics and morphodynamics in the highly altered North Branch of the Changjiang Estuary

Qi Zhang<sup>1</sup>, Daidu Fan<sup>1\*</sup> , Tao Feng<sup>2</sup>, Junbiao Tu<sup>1</sup> and Xingjie Guo<sup>1,3</sup>

## Abstract

The estuary is highly dynamic and sensitive to external and internal forcing. We examine a chain reaction of hydrodynamic and morphodynamic responses to a series of land reclamation projects during the period 1997 to 2017 in the North Branch of the Changjiang Estuary through the Digital Elevation Model (DEM) comparison and the numerical simulation by the Finite Volume Community Ocean Model (FVCOM). The results show that tidal amplification was further strengthened by the artificially reduced channel volume in the middle and upper segments of the North Branch due to the implementation of several large-scale land-reclamation projects in the first stage (1997–2007), and the channel siltation in the middle and upper segments was in turn further promoted by the increased tidal flows with flood dominance. In the second stage (2007–2017), tidal amplification was relaxed by the channel narrowing project at the lower segment and the waterway improvement project through channel dredging works at the middle and upper segments. Contemporary erosion volume was almost balanced by the accretion volume in the North Branch because of the weakening dominance of flood over ebb flows. Spatiotemporal variation in channel accretion and erosion patterns in response to estuarine engineering projects was vividly mirrored by the change of simulated bed shear stress in that the areas with increased (decreased) bed shear stress underwent severe erosion (accretion). These findings highlight again the dynamic feature of tide-dominated estuaries and the importance of simulation tools to the estuarine management.

**Keywords:** Changjiang estuary, Land reclamation, Hydrodynamic, DEM, FVCOM

## 1 Introduction

An estuary is the transition zone between the river and the sea with complex interactions of river runoff, wave, and tide. Estuaries play a key role in transferring terrestrial and marine materials to support typical ecosystems, which are increasingly vulnerable to human influence because of rapid socioeconomic development (Syvitski and Saito 2007; Fan et al. 2019; Kuenzer et al. 2020; Zhan

et al. 2020). A variety of human activities can be listed, e.g., dam construction, navigational work and dredging, land reclamation, groundwater extraction, and fossil resource exploitation (Anthony et al. 2015; Fan et al. 2017, 2021; Ve et al. 2021). Sediment discharge from numerous rivers in the world has decreased dramatically in recent decades in the context of global climate change and increasing human activities. These human activities have reduced the setting velocity of sediment and even caused erosion in some areas (Syvitski et al. 2005; Jiang et al. 2018). By profiling risk and sustainability in coastal deltas of the world, Tessler et al. (2015) concluded that human beings need to implement long-term

\*Correspondence: ddfan@tongji.edu.cn

<sup>1</sup> State Key Laboratory of Marine Geology, Tongji University, Shanghai 200092, China

Full list of author information is available at the end of the article

countermeasures for sustainable development to protect deltas. We should continuously strengthen our capability of estuarine research and predicting the development of estuarine deltas.

With rapid socio-economic development, land reclamation has become an important way to expand land space in coastal cities and countries. The intense tidal flat utilization directly or indirectly changes the original morphology and natural physical and chemical processes of the coastal zone (Muller et al. 2020; Tian et al. 2016). It also changes the dynamic geomorphology pattern of estuaries and increases the potential risks of the coastal zone. Estuarine engineering projects have been widely reported to exert instant impacts on hydrodynamics, and morphodynamics, consequently attracting intensive research attention (Park and Park 1998; Li 2010; Shin et al. 2019; Guo et al. 2021).

Altered estuaries have been widely evaluated by both field observations and numerical modeling. Van der Spek (1997) simulated hydrodynamic changes after reclamation and dam construction in the Scheldt Estuary based on a one-dimensional numerical flow model, demonstrating that increased tidal velocity together with the decreased predominance of flood tidal current in response to the reclamation projects resulted in enhanced siltation in the waterways. Nnafie et al. (2018) employed the Delft3D model to simulate the decadal evolution of estuarine channels by the reclamation of secondary basins in the Western Scheldt Estuary, elucidating that the lateral displacement of channels was triggered by the closure of secondary basins. Shen et al. (2018) used the FVCOM Surface Wave Module to simulate the influence of reclamation on saltwater intrusion and storm surge in the Pearl River Estuary, showing that tidal velocity and direction in the narrowed waterways were obviously changed by the engineering projects. Based on the FVCOM simulating results, Lu et al. (2015) discussed the influence of shoreline change on estuarine hydrodynamics after large-scaled land reclamations in the Qiantang River Estuary and the southern bank of Hangzhou Bay, proposing that the ports in the bay will face the tolerant siltation issue.

The North Branch had ever been the main waterway of the Changjiang Estuary with a river runoff split ratio larger than 50% before the 1840s, but the split ratio has declined to ~25% in the 1910s, and then to <5% after the 1950s (Wu et al. 2016b; Zhang et al. 2007; Obodoefuna et al. 2020). Meanwhile, the morphodynamics of the North Branch has changed obviously from a broad runoff-dominated distributary channel into a tide-dominated funnel-shaped estuary. The upstream entrance of the North Branch has undergone sustained obstruction by growing sandbars and shoals and their ultimate reclamation by annexing to

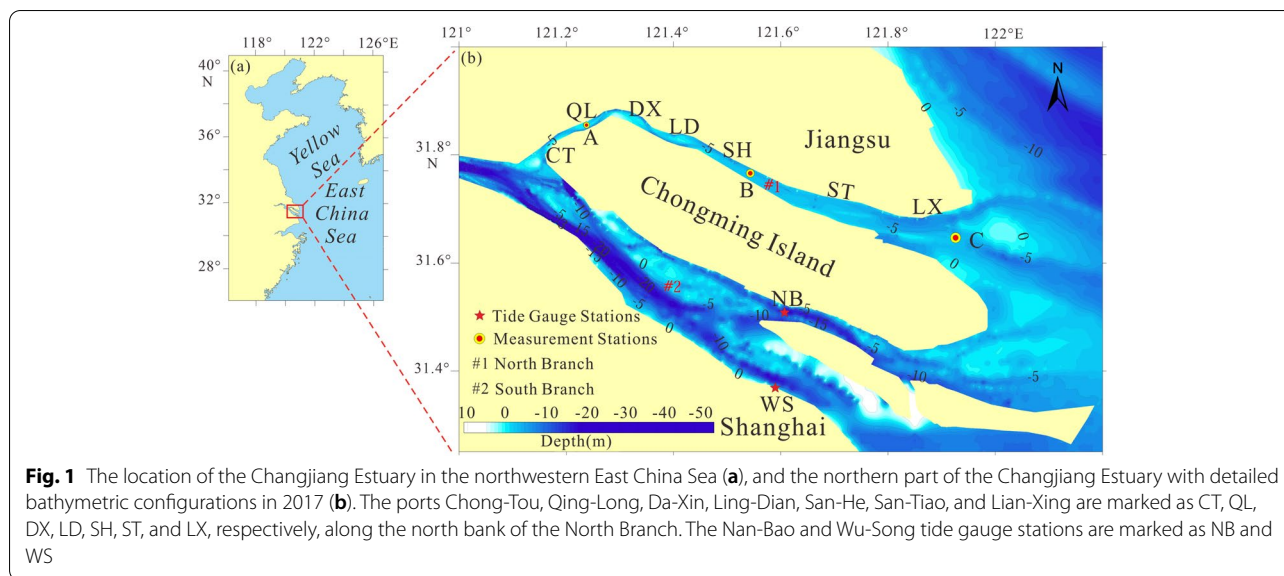
Jiangsu mainland or Chongming Island (see Fig. 9 in Obodoefuna et al. 2020). These processes have not only narrowed the entrance sharply but also increased the angle of incoming flow into the North Branch, and both retard the river runoff entering the North Branch (Dai et al. 2011; Zhang et al. 2019a, 2019b; Obodoefuna et al. 2020). Many researchers have studied the spatiotemporal variations in subaqueous channel configurations using time-series DEM data reconstructed from bathymetric maps (Dai et al. 2016). In the past 30 years, the reclamation area of the North Branch has reached 200 km<sup>2</sup>, resulting in an average annual shrinkage rate of 1.1% in terms of water area (Wu and Tong 2017). The channel volume below the 0 m has been reduced by about  $7.11 \times 10^8$  m<sup>3</sup> since 1990 by large-scaled reclamation projects in the North Branch (Yang et al. 2016). Consequently, the hydrodynamics in the North Branch has been significantly altered by these engineering projects, evolving from a mixed fluvial-and-tide-dominated distributary into a pure tide-dominated estuary (Li 2006). However, the controlling mechanism of the changing hydrodynamics and morphodynamics has scarcely been investigated by numerical simulation.

This study first examines the detailed morphodynamic change in the North Branch based on the DEM data reconstructed from the bathymetric maps in 1997, 2007, and 2017, to disclose the extreme human impacts by implementing several large-scale reclamation projects. Then, changes in current fields and bottom shear stress are investigated by simulating results from the FVCOM model. We aim to better understand hydrodynamic and morphodynamic responses to recent engineering projects in the North Branch and to provide a scientific basis for future waterway planning and wetland protection.

## 2 Natural setting and present engineering projects

### 2.1 Natural settings

The North Branch is a gradually abandoned distributary channel in the Changjiang Estuary (Obodoefuna et al. 2020), which is divided from the South Branch by Chongming Island. It has a funnel shape in a planar view (Fig. 1). Before the 1840s, the North Branch was the main waterway of the Changjiang Estuary with >50% of annual river discharge. Tong-Hai sandbar and Jiang-Xin sandbar at the northwest entrance of the North Branch expanded and the associated secondary channels silted up rapidly in the first half of the twentieth century (Obodoefuna et al. 2020). After that, the main stream of the Yangtze Estuary into the sea was diverted to the South Branch, led to a sharp decline in the split ratio of water discharge into the North Branch, which was 25% in 1915 and 8.7% in 1958, respectively (Mao et al. 2014). Since the 1950s, the width of the river channel of the North Branch has been greatly



reduced due to the large-scale reclamation, implying a decreased river influence and a transformation from a river-dominated distributary channel into a tide-dominated estuary (Guo et al. 2022). The total channel length is about 84 km from Chong-Tou (CT) (near the upstream entrance) to Lian-Xing (LX) (close to the downstream outlet), which can be further divided into 3 segments in terms of channel morphodynamics (Ma et al. 2013). The upper segment is located between CT and Qing-Long (QL), featured by a narrow and shallow channel with tidal bores. The middle segment between QL and San-Tiao (ST) is characterized by dynamic migration of channel-bar/shoal complexes under strong tidal actions. The lower segment is a tidal waterway between ST and LX with an obvious increase in channel width and depth, where tidal channels, sand ridges, and muddy banks are well developed (Chen et al. 2011; Li et al. 2015; Obodoefuna et al. 2020).

The North Branch is dominated by semidiurnal tides, where the duration of ebb tides (>7 h) is significantly greater than that of flood tides (<4 h), consequently resulting in much larger velocities of flood flows than ebb flows (Li et al. 2015; Obodoefuna et al. 2020). Tidal ranges gradually increase upstream due to the convergent effect of a funnel shape, with average tidal ranges of 2.93 m at LX and 3.07 m at ST (Fan et al. 2004). Furthermore, when the semidiurnal tides with an apparent diurnal inequality shoot into the upstream narrowing and shallowing channel, the tidal wave energy converges and tidal fronts can be strongly deformed to produce tidal bores between Ling-Dian (LD) and QL (Wu et al. 2012; Li et al. 2016; Zhang et al. 2007). Tidal

current is the main driver of sediment transport and channel accretion/erosion change.

## 2.2 Reclamation and waterway-improvement projects

In the upper segment (CT to QL), two reclamation projects have been implemented in the last three decades with a total land area of 26.8 km<sup>2</sup> (Fig. 2). The reclamation of the Wei-Jiao sandbars along the north bank of the entrance greatly narrowed down the inflow channel, consequently reducing the river runoff entering the North Branch. This has been further deteriorated by the reclamation of the Chongtuo bank during 2000–2005, and thereafter the channel width was reduced to 1497 m.

In the middle segment (QL to ST), several reclamation projects were carried out to create a new land area of 58 km<sup>2</sup> through the reclamation of Xing-Yue sandbar, Ling-Dian sandbar, Yong-Long sandbar, and Xin-Long sandbar, together with damming a tidal channel to form the freshwater Beihu Lake with an area of 32.9 km<sup>2</sup> (Fig. 2). In the lower segment (ST to LX), a cumulative area of 80.3 km<sup>2</sup> has been reclaimed from the northeastern bank of Chongming Island since 1981. In addition, the channel narrowing project by land reclamation along the southern bank in the middle and lower segments was implemented from 2005 to 2015 to alleviate channel siltation and saltwater intrusion in the North Branch (Yang et al. 2016; Zhang et al. 2019a, 2019b). The estuarine projects in the North Branch can be divided into two stages: land reclamation projects in the middle and upper segments in the period 1997–2007, and the channel narrowing project in the middle and lower segments plus channel dredging activities in the period 2007–2017.

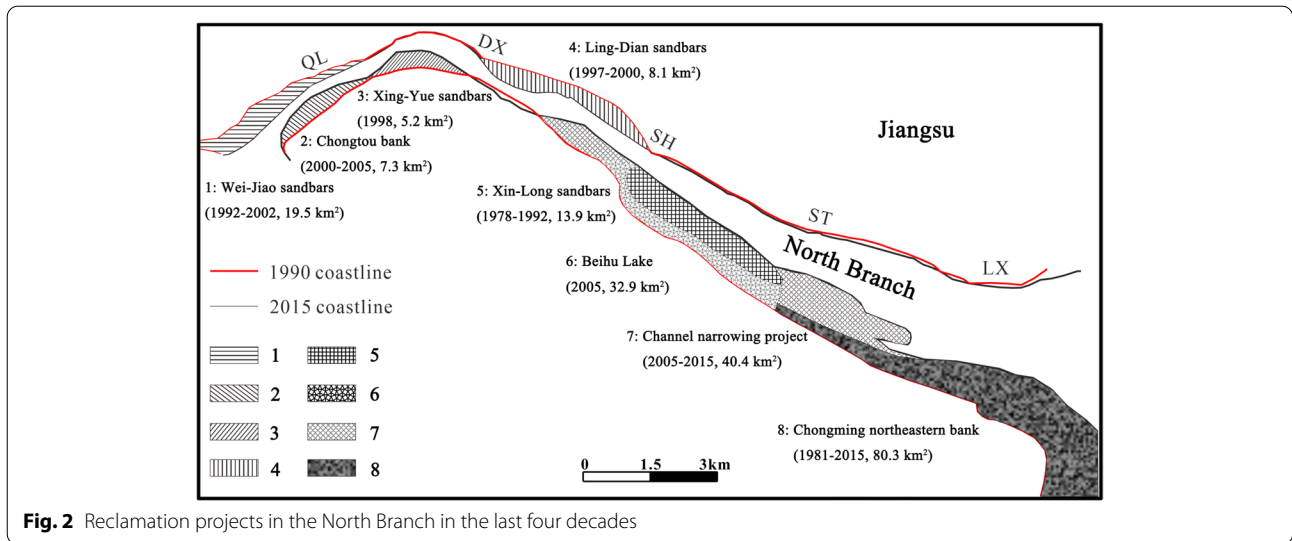


**Fig. 2** Reclamation projects in the North Branch in the last four decades

### 3 Methods

#### 3.1 Establishment of DEM

In order to study the topographic evolution characteristics of estuaries, a quantitative topographic research method has been developed. The method is to build a digital elevation model (DEM). We can more accurately understand the details of underwater topographic changes through DEM comparison, so as to further explore the reasons and mechanisms of its changes. In this paper, high-resolution bathymetric data of 1997, 2007, and 2017 are collected from Shanghai Institute of Geological Survey. The maximum and minimum errors of plane positioning are  $\pm 1.99$  m and  $\pm 0.95$  m. All water-depth data are normalized to the theoretically lowest astronomical tidal datum at Wusong (WD), and their geographical positions are referenced to the same coordinate of Beijing 54. Kriging interpolation was used for the generation of DEM of the study area. Surfer software can output the isobath of the DEM in different years and the topographic changes of a certain section. Using the Math tool can add and subtract data files of different years. The contour map drawn by the grid file after the subtraction operation is the erosion/accretion map. The Volume tool can calculate the siltation and scouring volume and net change over a period of time. The DEM data of 1997, 2007, and 2017 were used to calculate the channel volume below 0 m in different years, and the two consecutive different years of DEM data were compared to denote erosion and siltation patterns and their volumes in the upper, middle and lower segments, respectively. The cross-section area and channel width of a few selected profiles were consequently calculated.

#### 3.2 Model configuration

In this study, the ocean hydrodynamic model FVCOM (Finite-Volume Community Ocean Model) is used to simulate the flow field of the North Branch and its adjacent water. FVCOM adopts unstructured triangular high-resolution mesh in the horizontal direction to represent the complex coastlines of the Changjiang Estuary and sigma coordinates in the vertical direction to describe the complex bottom topography of part of the Yellow Sea and the East China Sea. The numerical method uses the finite-volume approach, which combines the best attributes of finite-element methods for geometric flexibility and finite-difference methods for simple discrete coding and computational efficiency. This numerical approach also provides a much better representation of mass, momentum, salt, and heat conservation in coastal and estuarine regions with complex geometry (Chen et al. 2012; Qi et al. 2009; Yang and Khangaonkar 2009).

The governing calculations consist of the following momentum, continuity, temperature, salinity, and density equations:

$$\frac{\partial Du}{\partial x} + \frac{\partial Dv}{\partial y} + \frac{\partial w}{\partial \sigma} + \frac{\partial \zeta}{\partial t} = 0 \tag{1}$$

$$\frac{\partial Du}{\partial t} + \frac{\partial Du^2}{\partial x} + \frac{\partial uv}{\partial y} + \frac{\partial uw}{\partial \sigma} = fDv - gD \frac{\partial \zeta}{\partial x} + \frac{\partial}{\partial \sigma} \left( \frac{K_M}{D} \frac{\partial u}{\partial \sigma} \right) \frac{gD}{\rho_0} \left[ \frac{\partial}{\partial x} \left( D \int_{\sigma}^0 \rho d\sigma' \right) + \sigma \rho \frac{\partial D}{\partial x} \right] + DF_x \tag{2}$$

$$\frac{\partial Dv}{\partial t} + \frac{\partial Duv}{\partial x} + \frac{\partial v^2}{\partial y} + \frac{\partial vw}{\partial \sigma} = fDu - gD \frac{\partial \zeta}{\partial y} + \frac{\partial}{\partial \sigma} \left( \frac{K_M}{D} \frac{\partial v}{\partial \sigma} \right) \frac{gD}{\rho_0} \left[ \frac{\partial}{\partial y} \left( D \int_{\sigma}^0 \rho d\sigma' \right) + \sigma \rho \frac{\partial D}{\partial y} \right] + DF_y \tag{3}$$

$$\frac{\partial P}{\partial z} + \rho Dg = 0 \tag{4}$$

$$\rho = \rho(T, S) \tag{5}$$

$$\begin{aligned} \frac{\partial DT}{\partial t} + \frac{\partial DuT}{\partial x} + v \frac{\partial DvT}{\partial y} + \frac{\partial \omega T}{\partial \sigma} \\ = \frac{1}{D} \frac{\partial}{\partial \sigma} \left( K_h \frac{\partial T}{\partial \sigma} \right) + D\hat{H} + DF_T \end{aligned} \tag{6}$$

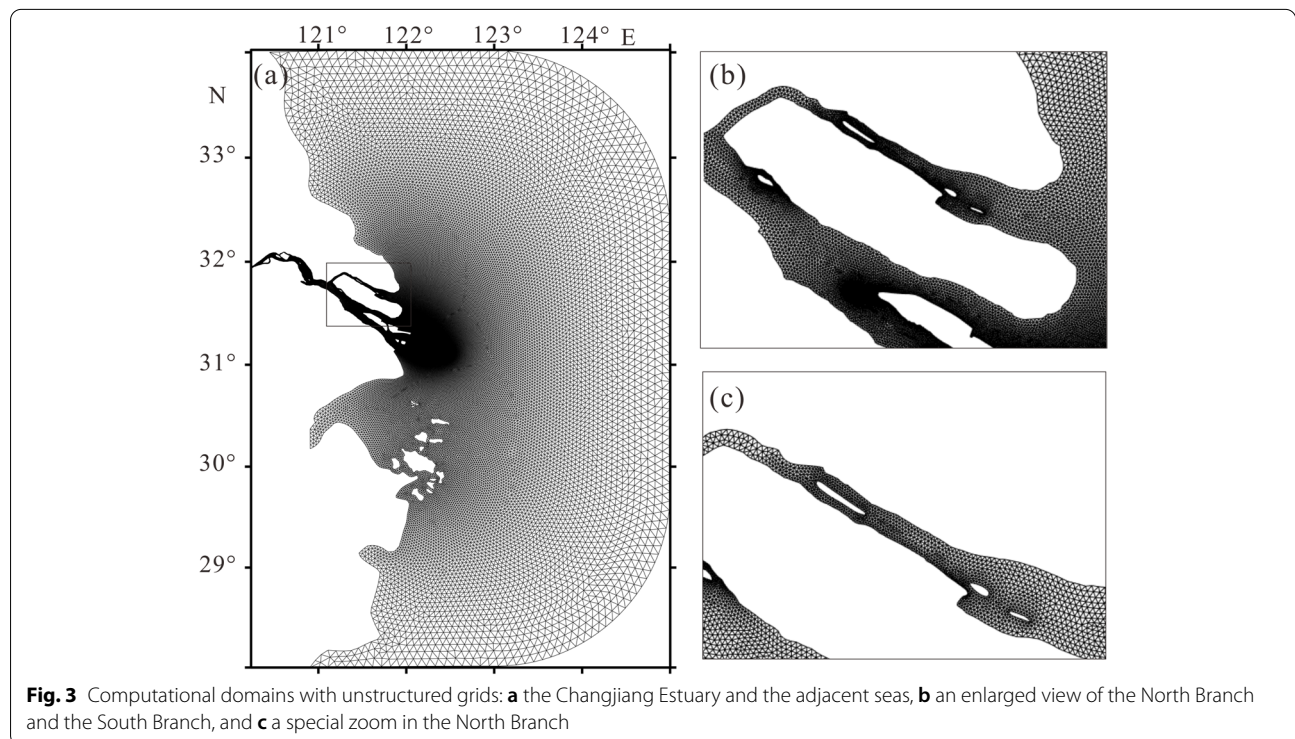
$$\frac{\partial DS}{\partial t} + \frac{\partial DuS}{\partial x} + v \frac{\partial DvS}{\partial y} + \frac{\partial \omega S}{\partial \sigma} = \frac{1}{D} \frac{\partial}{\partial \sigma} \left( K_h \frac{\partial S}{\partial \sigma} \right) + DF_S \tag{7}$$

Where  $u$ ,  $v$ , and  $w$  are the  $x$  (east),  $y$  (north),  $\sigma$  (vertical) velocity components;  $\sigma$  varies from  $-1$  at the bottom to  $0$  at the surface;  $t$  is the time;  $D$  is the total water column depth,  $D=H+\zeta$ ,  $H$  is the bottom depth,  $\zeta$  is the height of the free surface;  $T$  is the temperature;  $S$  is the salinity;  $\rho$  is the density;  $P$  is the pressure;  $f$  is the Coriolis parameter;  $g$  is the gravitational acceleration;  $K_m$  is the vertical eddy viscosity coefficient; and  $K_h$  is the thermal vertical eddy diffusion coefficient;  $F_x$ ,  $F_y$ ,  $F_T$  and  $F_S$  represent the horizontal momentum, thermal, and salt diffusion terms (Wan et al. 2016).

The computational domain of this model covers the Changjiang Estuary, Hangzhou Bay, and Zhoushan Island Complex, and is bounded by an open boundary in the

inner shelf of the East China Sea. The upper boundary of the river is located near the tidal limit at Datong. The model domain is composed of 148,821 triangular elements and 75,464 triangular nodes. The horizontal resolution (measured by the shortest line of a triangle) gradually increases from the outer sea boundary to the estuary, and varies from 0.2 km inside the North Branch to 1.0 km in the open boundary (Fig. 3). The vertical resolution is determined by 20 uniform sigma layers. The Mellor and Yamada level 2.5 (MY-2.5) and Smagorinsky turbulent closure schemes are used for vertical and horizontal mixing. The external and internal mode time steps are 1.0 s and 4.0 s, respectively. Model bathymetric data of the North Branch are reconstructed from the nautical charts in 1997, 2007, and 2017. The flow field in the study area is mainly influenced by the combined effect of tidal currents and runoff, and the input conditions of three numerical experiments are the same. The model is driven by five major tidal constituents ( $M_2$ ,  $S_2$ ,  $N_2$ ,  $O_1$ , and  $K_1$ ) at the offshore open boundary, and the tidal amplitude and phase are obtained by interpolating FES2014 global tidal model. The upstream river boundary data use the annual average runoff at Datong station. The calculation time is 30 d, including the spring, moderate, and neap tides.

Continuous tripod measurements of flow velocity in the near-bottom boundary layer were collected from three stations (Station A, B and C) between September 28 and October 5, 2018 (Fig. 1). The current data



were measured by acoustic Doppler velocimeter (ADV) deployed by a bottom mounted tripod. The sampling frequency of ADV was 16Hz. ADV was deployed at 0.55 m above the bed at Station A, 0.6 m above the bed at Station B and C. We also obtained the tidal level in 2018 from the tide gauge stations at Nan-Bao and Wu-Song. Both data were used to test model performance (Fig. 4). The flow velocity at station A is about 0–0.2 m/s, while that at station B and C is about 0–1.2 m/s. The reason for the smaller flow velocity at station A may be due to the fact that the flow velocity was measured during the neap tide condition and region close to bed. In addition, while station A is located from QL to CT where the north and south branch flood tidal currents meet. This area is controlled by the weakening of tidal flows, the flow velocity is lower (Dai et al. 2016).

To further quantify the accuracy of the model results, a statistical analysis of the root mean square error (RMSE) was performed, which can be expressed by the following equation (Ralston et al., 2010):

$$RMSE = \sqrt{\frac{\sum_{i=1}^n (O_i - P_i)^2}{n}} \tag{8}$$

Where  $O_i$  and  $P_i$  are model simulated and actual observed values and  $n$  is the number of statistical

variables. The RMSE between the observed and modeled flow velocity at stations A, B and C ranges from 0.03 to 0.12 m/s (Table 1). The RMSE of flow direction is 16° and 37° for station A and Station B, respectively. The RMSE of tidal level is also small with an average of about 0.21 m. Overall, our model captures the prevalent trends in flow velocity, flow direction and tidal level, giving confidence to the model application to investigate the hydrodynamic processes in the study area.

## 4 Results

### 4.1 Variations in channel morphological features along the north branch

The water depth in the North Branch is generally not deeper than 14 m with the most frequent depths between

**Table 1** The root mean square error (RMSE) between the observed and modeled data of flow velocity, flow direction, and tidal elevation

Station	Velocity	Direction	Station	Tidal level
A	0.03	37.46	Nan-Bao	0.19
B	0.12	15.84	Wu-Song	0.23
C	0.11	34.90	/	/

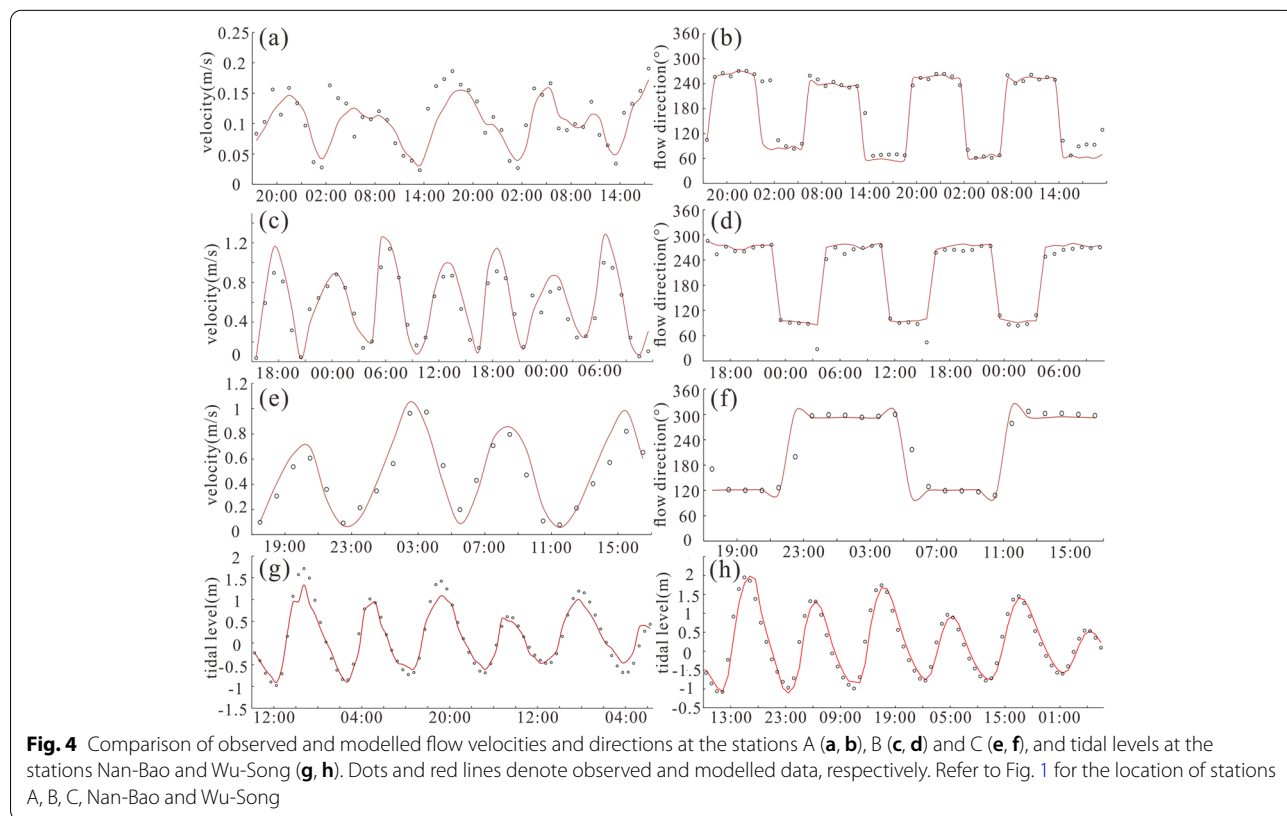


**Fig. 4** Comparison of observed and modelled flow velocities and directions at the stations A (a, b), B (c, d) and C (e, f), and tidal levels at the stations Nan-Bao and Wu-Song (g, h). Dots and red lines denote observed and modelled data, respectively. Refer to Fig. 1 for the location of stations A, B, C, Nan-Bao and Wu-Song

5 m and 2 m, and it is usually less than 2 m in the upper segment (Fig. 5a, b, c). Recent reclamation projects have significantly changed channel morphology, and the change in terms of channel width and cross-section area varied over different segments. Due to land reclamation between 2000 and 2005, the channel width along the CT profile decreased from 2304 m in 1997 to 1497 m in 2007 with a narrowing rate of 40%, and its cross-section area was reduced by 86% from 8905.12 m<sup>2</sup> in 1997 to 1172.71 m<sup>2</sup> in 2007 (Figs. 5d, and 6a). While, the cross-section area of CT increased by 20% from 2007 to 2017 due to the waterway improvement project. The channel width of QL and DX has little changed in the past 20 years, but their cross-section area changed obviously with similar patterns of CT. The channel width of SH in the middle segment decreased from 4109 m in 1997, through to 3203 m in 2007, and then to 1882 m in 2017, with a cumulative narrowing rate

of 63.3% which is the highest change in the whole North Branch. The channel width and cross-section area of ST in the lower segment changed slightly for the period 1997–2007, but they decreased by 50% and 56% between 2007 and 2017, respectively, mainly resulting from the implementation of channel narrowing project in the period 2005–2015 (Fig. 2). The channel width of LX near the outlet of the North Branch decreased from 10,822 m in 1997, through to 9701 m in 2007, and then to 7505 m in 2017.

The channel volume below 0 m in the North Branch decreased by half from 1434 × 10<sup>8</sup> m<sup>3</sup> in 1997 to 734 × 10<sup>8</sup> m<sup>3</sup> in 2017, but majorly occurred in the first decade 1997–2007 (Table 2). In the upper segment, an overall trend of siltation was indicated between 1997 and 2007 by a 68.66% reduction in the channel volume, but it was followed by slight erosion during 2007–2017 resulting from the waterway improvement project. Similar to the

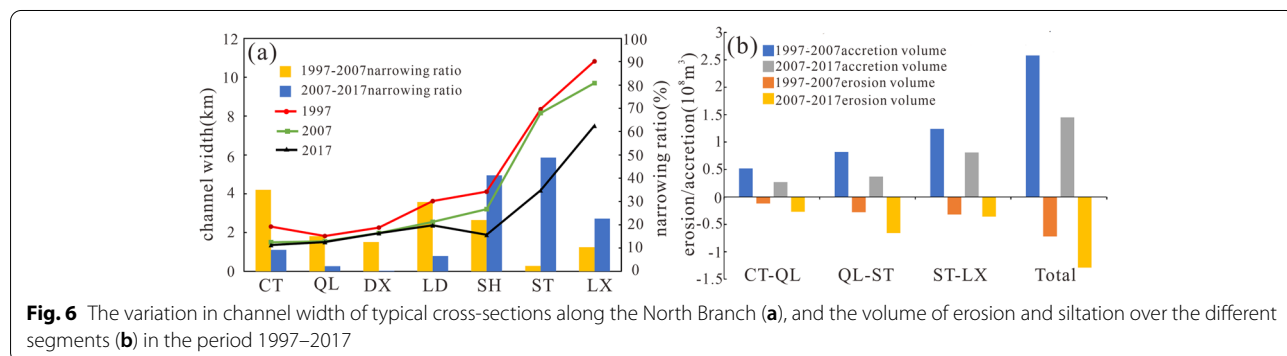
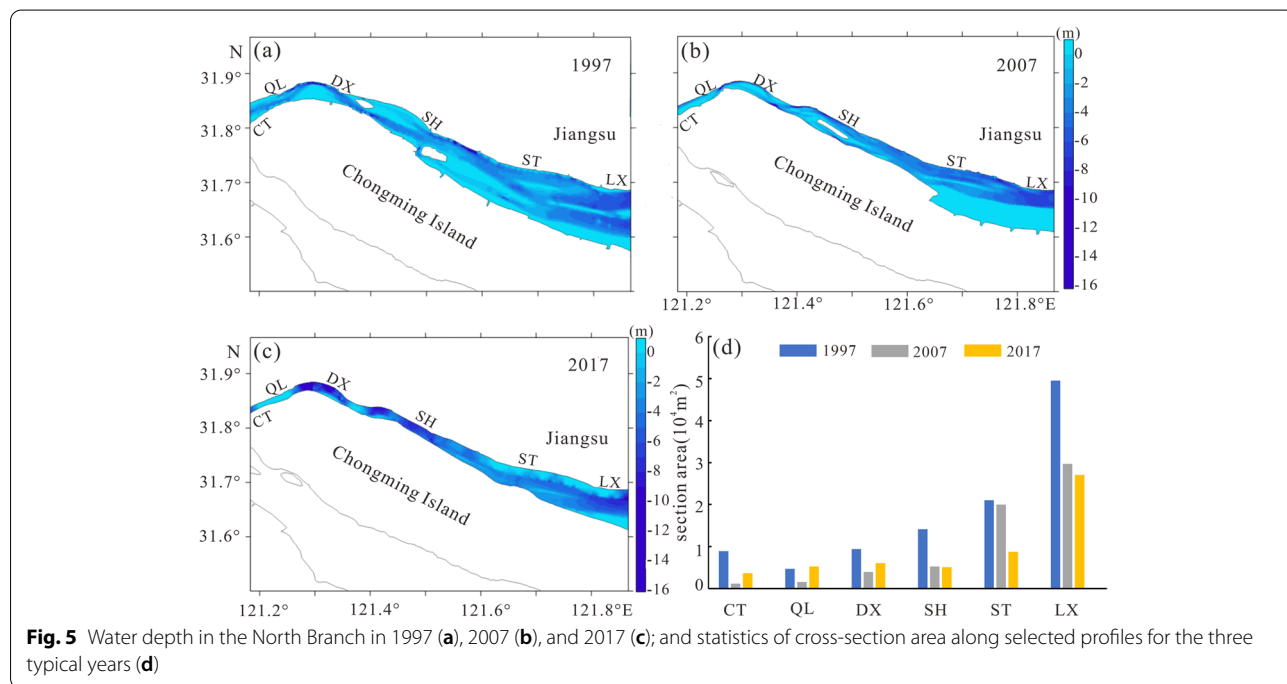


**Table 2** The statistics of channel volume below 0m over different segments of the North Branch and their variation rates over the two study periods

Channel volume and variation rate	CT-QL	QL-ST	ST-LX	Total
Volume in 1997/10 <sup>8</sup> m <sup>3</sup>	0.67	5.69	7.98	14.34
Volume in 2007/10 <sup>8</sup> m <sup>3</sup>	0.21	2.62	4.65	7.48
Volume in 2017/10 <sup>8</sup> m <sup>3</sup>	0.3	2.86	4.28	7.34
Variation rate in 1997–2007/%	−68.66	−53.95	−41.73	−47.84
Variation rate in 2007–2017/%	42.86	9.16	−7.96	−1.87

upper segment, the channel volume in the middle segment decreased by 53.95% between 1997 and 2007 but increased by 9.16% between 2007 and 2017. The channel volume of the lower segment decreased continuously by 41.73% in 1997–2007 and 7.96% in 2007–2017. Siltation in the lower segment has been highly alleviated at the later stage due to the implementation of the channel-narrowing project, which will be further discussed in the section 4.3.

**4.2 Simulated variations in average tidal level and flow velocity**

The average high and low tidal levels (Fig. 7) and average flood and ebb flow velocities (Fig. 8) at six typical sections are calculated from the simulated tidal current

fields in 1997, 2007, and 2017, respectively, using the FVCOM model.

The average high tide level in the North Branch rose meanly by 0.12 m in the period 1997–2007, and a higher increase was observed in the middle segment than the others (Fig. 7a). Contemporarily, the average low tide level descended at different extents with a largest descending magnitude of 0.5 m between SH and ST (Fig. 7b). However, the average high tide level dropped significantly in the period 2007–2017 with a maximum drop of 0.21 m at DX and a minimum drop of 0.04 m at LX (Fig. 7a). At the same time, the mean low tide level changed little, with a slight rise at LD and a drop of 0.11 m at SH (Fig. 7b).

The average flood and ebb flow velocities were simulated to increase significantly in the middle and upper segments but decrease in the lower segment in the period 1997–2007 (Fig. 8). The maximum increase of average flood flow velocity occurred at SH from 1.12 m/s to 1.38 m/s, and for the average ebb flow velocity at LD from 1.21 m/s to 1.48 m/s. During 2007–2017, the middle and upper segments mainly showed a decrease in the average flood flow velocity and a general increase in the average ebb flow velocity, with the inverse patterns occurred in the lower segment (Fig. 8).

**4.3 Simulated variations in bed shear stress**

Spatiotemporal variations in channel erosion and siltation patterns of the North Branch are disclosed by

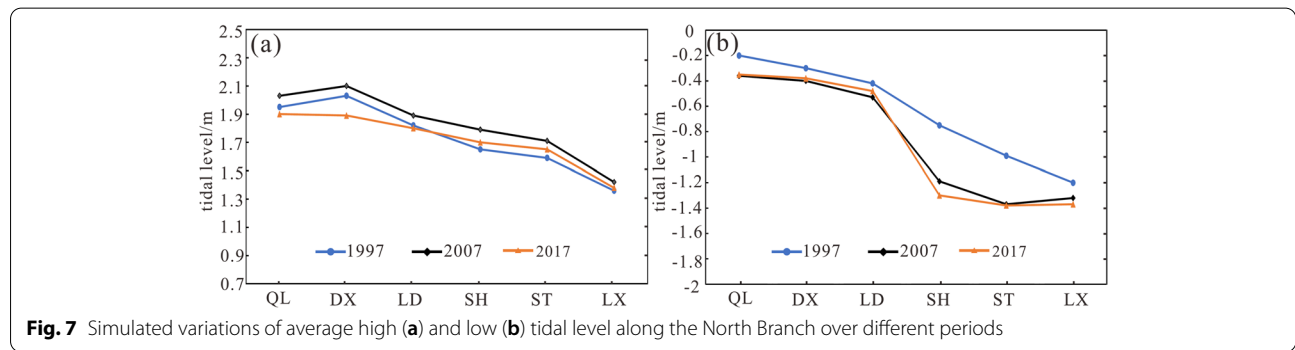


**Fig. 7** Simulated variations of average high (a) and low (b) tidal level along the North Branch over different periods

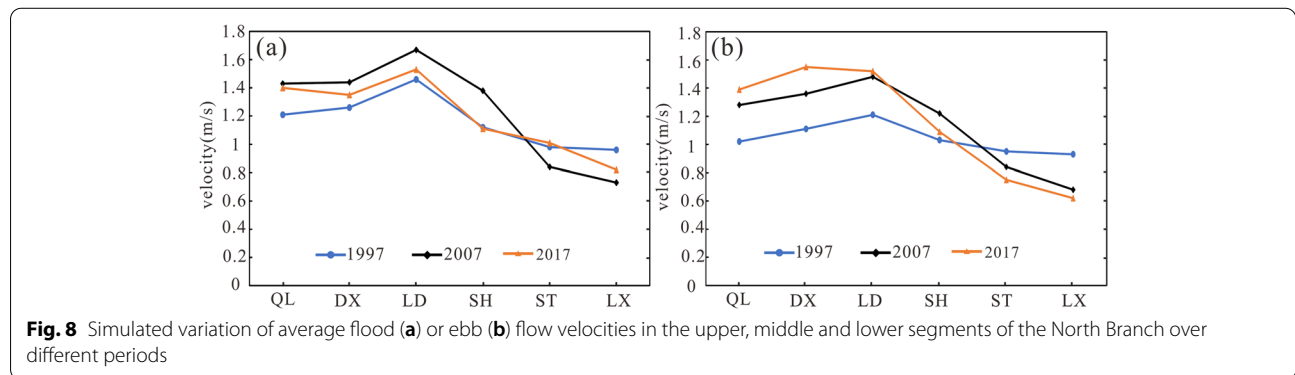


**Fig. 8** Simulated variation of average flood (a) or ebb (b) flow velocities in the upper, middle and lower segments of the North Branch over different periods



comparing two consecutive different years of DEM data (Fig. 9a, b). During 1997–2007, most of the southern bank underwent rapid accretion with peak accretion in the lower segment, while the northern bank experienced severe erosion except for the section near DX (Fig. 9a). Most of accretional banks and shoals had been reclaimed for land, and channel erosion and siltation patterns were therefore obviously changed in the following period 2007–2017. Severe erosion occurred at the upstream entrance, the upper part of the middle segment, and the southern half of the lower segment (Fig. 9b). The erosion volume was almost balanced by the accretion volume in the whole channel of North Branch during 2000–2017 after the implementation of the channel narrowing project and the waterway improvement project to strengthen tidal flows for reducing siltation in the main channel. This was in a sharp contrast with the previous period (1997–2007) when almost a half of channel volume was erased by natural accretion and land reclamation.

The controlling mechanism for obvious changes in channel erosion and accretion patterns are further explored by simulating bed shear stress variations in response to the implementation of large-scale estuarine projects in the North Branch. Bed shear stress is an important indicator of estuarine sediment dynamics and morphodynamics (Zhu et al. 2014). We mainly consider the bed shear stress induced by tidal currents because the North Branch is dominated by strong tides with negligible wave actions in the long and narrow estuarine stretch between LX and CT (Li et al. 2016). Theoretically, the bed shear stress by tidal currents is proportional to

the magnitude of tidal current velocities, which can be expressed by the following equations (Stanev et al. 2009; Wilcock 1996):

$$\tau_{bx} = C_f \rho |U|u \tag{9}$$

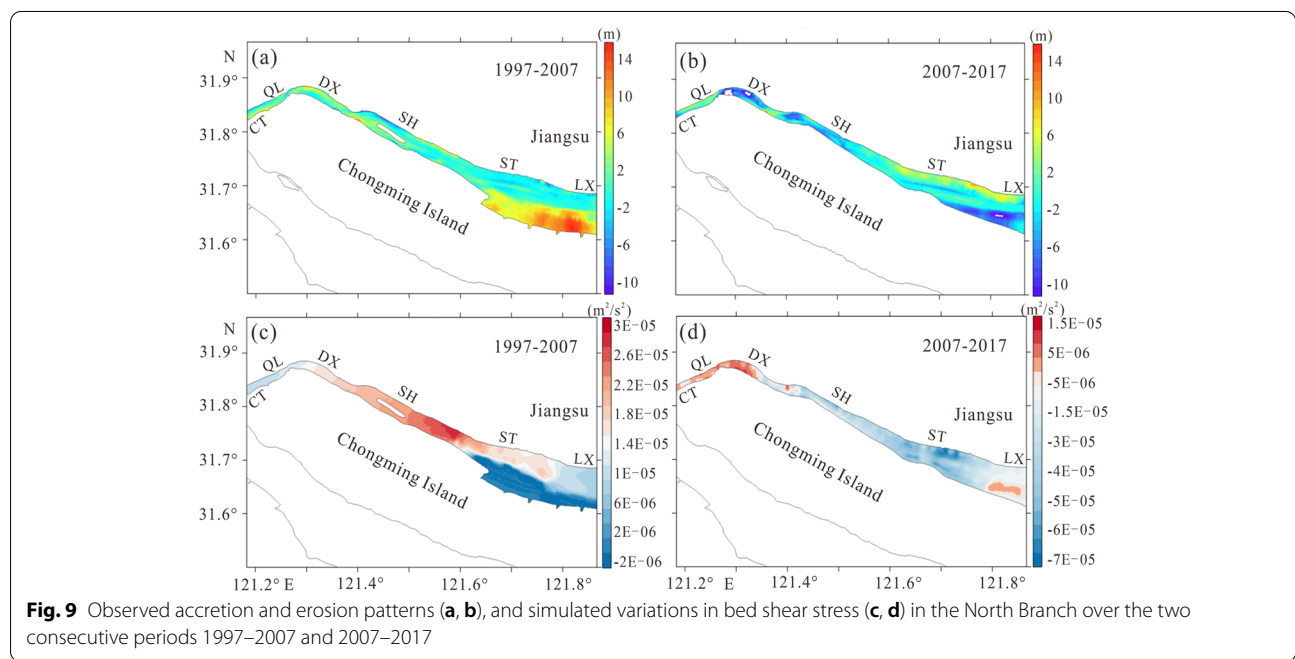
$$\tau_{by} = C_f \rho |U|v \tag{10}$$

Where  $\rho$  is the density and  $C_f$  is the bottom friction coefficient. We first simulated spatial variation of bed shear stress in the North Branch in the three typical years by the setting-up FVCOM model as described in the section 3. Then, the two consecutive years of the modelling results are compared to disclose their varied patterns in response to the contemporary channel morphological change. It is clearly shown that the areas with increased bed shear stress (positive values in Fig. 9c, d) underwent severe erosion, and vice versa for the areas having decreased bed shear stress (negative values) where obvious accretion occurred (Fig. 9).

## 5 Discussion

### 5.1 Impact of estuarine projects on the hydrodynamics and bed shear stress in the north branch

The North Branch has been gradually abandoned since the middle nineteenth century, and its runoff split ratio had decreased from > 50% before the 1840s to < 5% after 1950s. Consequently, fluvial sediment supply from the upstream entrance of the North Branch had sharply declined to a negligible level, but offshore sediment



input by tides is very huge to support rapid siltation in the channel (Dai et al. 2016; Obodoefuna et al. 2020). In another word, recent morphodynamic change in the North Branch has little been influenced by the sharp decrease of river sediment discharge due to constructing numerous reservoirs in the upstream drainage basin, but it is highly sensitive to local hydrodynamic change induced by large-scale land reclamation and waterway improvement projects within the North Branch.

Trumpet morphology is generally known to favor tidal amplification in the estuary as that has occurred in the North Branch. Land reclamation was mainly implemented in the middle and upper segments during the period 1997–2007, resulting in significant reduction of the channel width above ST (Fig. 6a). Following this channel morphological change, tidal range was simulated to increase on average by 0.42 m in the same period with a maximum increase between LD and ST (Fig. 7). The average velocities of flood and ebb flows above ST were modelled to increase by 0.22 m/s and 0.24 m/s, respectively, while they decreased by 0.19 m/s and 0.18 m/s in the lower segment which should be related to its relative wide channel with less change in the period 1997–2007 (Fig. 8).

During 2007–2017, the channel narrowing project was carried out principally by reducing the channel width of the middle and lower segments in order to relax tidal amplification by the funnel shape (Fig. 6a). Together with the waterway improvement project by dredging along the main channel, tidal amplification was weakened as shown by simulated decrease in tidal ranges in the North Branch (Fig. 7). Contemporarily, the predominance of flood flows over ebb flows was significantly reduced (Fig. 8), unfavorable for landward sediment transport to support siltation in the North Branch as observed previously. Moreover, the upper segment was simulated to change from a flood dominance into an ebb dominance status, favoring the seaward sediment transport to induce channel erosion. Such change also relaxes the saltwater spilling over from the North Branch into the South Branch as one of main targets for the channel narrowing project.

The bed shear stress is related to velocity and bottom drag coefficient (BDC) in Eq. (9) and (10). Where, BDC is affected by water depth, depth averaged tidal current velocity, topography and sediment type (Qian et al. 2021). Due to the influence of shallow water depth and reclamation projects in the North Branch, the bottom friction coefficient in this area presents complex spatial and temporal pattern. The bottom friction coefficient of the middle and upper segments is generally larger than that of the lower segment (Lyu and Zhu 2018). The increase of the bed shear stress in the upper segment is mainly related to the increase of the flow velocity at the entrance

(Fig. 9c). The decrease of the bed shear stress in the middle segment is mainly related to the decrease of the flow velocity and shallower water depth (Fig. 9d).

## 5.2 Impact of engineering projects in different estuaries

With the rapid coastal economical and societal development, land reclamation has become an important way to meet for a strong dire for land resources (Fan et al. 2013; Teng et al. 2021). The effects of engineering projects on estuarine hydrodynamics, sediment-dynamics and morphodynamics have been extensively reported, showing some similar mutual controlling mechanisms with different magnitudes.

The Western Scheldt Estuary in the Netherlands has been affected by human activities since the beginning of seventeenth century, dominated by land reclamation and damming before 1950 and then mainly by channel dredging. Reclamation led to a reduction of the intertidal area from 295 km<sup>2</sup> in 1650, through to 196 km<sup>2</sup> in 1800, then to 104 km<sup>2</sup> in 1950, and to 90 km<sup>2</sup> in 1968 (Stark et al. 2019; Dam et al. 2016; De Vriend et al. 2011; Van den Berg et al. 1996). The Western Scheldt Estuary has a unique multiple channel system, separated by narrow flood and ebb channels with intervening shoals at regular intervals (Van Veen et al. 2005). Similar to the North Branch, the main driver is tidal flows, with river runoff accounting for only 0.6% of the tidal prism. Reduction in the intertidal area by reclamation has led to decreasing in the maximum velocity of flood and ebb tides. Although the dominance of flood tide in the channel still maintains, its priority over ebb tide decreases significantly, consequently reducing landward sediment transportation (Van den Berg et al. 1996; Swinkels et al. 2009).

The Pearl River Estuary is characterized by the intricate network of tributary and distributary channels entering the open water. It has three main tributaries (the West, North, and East Rivers) which flow into the four open estuaries (Lingding Bay, Modaomen, Jitimen and Huangmao Bay) through eight outlets (Wu et al. 2006a; Zhang et al. 2010; Wu et al. 2016; Yang et al. 2020). Land reclamation from the Pearl River Estuary can be traced much earlier than the 1960s when large-scale reclamation projects were carried out to reclaim a total area of 334 km<sup>2</sup> during 1966–1996. These projects have significantly reduced the estuarine area and narrowed the distributary channels, leading to a reduction in the tidal prism which in turn promotes estuarine siltation including the development of shallow shoals in the distributary mouths (Zhang et al. 2015).

Large-scale reclamation projects have been implemented in the Qiantang River Estuary since the 1960s with an accumulative reclaimed area of about 733 km<sup>2</sup>, narrowing the estuarine channel width by 1/2 to 3/4

**Table 3** Impact of engineering projects in different estuaries

Estuaries	Main driver	Reclaimed area(km <sup>2</sup> )	Change of width(km)	Change of tidal range(m)	Net deposition (10 <sup>8</sup> m <sup>3</sup> )	References
Western Scheldt	Tide	205 (1650–1968)	−2.8 (1800–1980)	1.8 (1650–1968)	1.3 (1878–1970)	(Nnafie et al. 2018; Van den Berg et al. 1996; Van der Spek 1997)
Pearl River	Runoff	334 (1970–2000)	/	0.4 (1960–2000)	9.45 × 10 <sup>6</sup> (1970–2000)	(Zhang et al. 2015; Zhang et al. 2010; Shen et al. 2018)
Qiantang River	Tide	733 (1960–2000)	−12 (1960–2000)	0.13 (1960–2000)	52 (1959–2003)	(Han and Dai 2002; Xie et al. 2017; Xie et al. 2021)
North Branch	Tide	207.6 (1992–2015)	−1.9 (1997–2017)	0.22 (1997–2017)	2 (1997–2017)	/

(Han and Dai 2002; Ni and Lin 2003). The rapidly narrowing channel intensifies the reflection of tidal waves in the estuary to raise the high tide level and increase tidal range accordingly. The tidal prism in the upper estuarine section is drastically reduced, resulting in severe siltation in the channel (Xie et al. 2009; Xie et al. 2021; Xie et al. 2017).

A comparison of the impacts of the estuarine projects in the Western Scheldt Estuary, Pearl River Estuary, Qiantang River Estuary, and the North Branch of the Changjiang Estuary reveals certain commonalities (Table 3). The reclamation of coastal mudflats has transformed natural tidal flats, which used to store and dissipate tidal energy, into artificial shores, narrowing the river width and changing the water level, tides and geomorphology of the estuary. The reduction of the total water area after reclamation leads to the reduction of tidal prism, the reduction of tidal momentum, the reduction of sand-carrying capacity, and the easier siltation of the estuary. In summary, estuarine projects like land reclamation could obviously change hydrodynamic boundary, producing a chain reaction of sediment-dynamics and morphodynamics. It should be cautious to plan and implement any estuarine projects and their adverse effects should be comprehensively evaluated using monitoring and simulation methods before and after the projects.

## 6 Conclusions

The North Branch in the Changjiang Estuary has long evolved from a runoff-dominated distributary channel into a pure tide-dominated estuary. Recently, the channel morphology has been significantly changed by large-scale engineering projects in the estuary, consequently inducing spatiotemporal variations in hydrodynamics, sediment-dynamics and morphodynamics as shown by both observational and simulated results.

The channel volume below 0 m was reduced by half due to the reclamation of rapidly accretional muddy banks and sandy shoals/ridges mainly in the upper and middle

segments during 1997–2007. This further strengthened tidal amplification due to the narrowing effect of upper trumpet estuary, as shown by simulated increase of tidal ranges and current velocities of flood and ebb tides, typically in the middle segment. Flood dominance was maintained in the main channel, favoring upstream sediment transport to promote siltation in the upper segment. Bed shear stress in the southern half channel of the lower segment was simulated to weaken obviously in the shadow of a large-scale reclamation project, in high accordance with contemporary peak accumulation distribution pattern therein.

To reduce siltation in the middle and upper segments of the North Branch, a channel narrowing project was carried out by reclaiming the broad accretional muddy bank at the lower segment together with the waterway improvement project during 2007–2017. Consequently, tidal amplification was relaxed as demonstrated by simulated decrease in tidal ranges and the less predominance of flood flows over ebb flows. Typically, the main channel in the upper segment has shifted from flood into ebb dominance to induce erosion therein. In all, the contemporary erosion volume was almost balanced by the accretion volume in the whole North Branch channel.

### Acknowledgements

We appreciate Prof. Qinghe Zhang (Tianjin University, China) and Dr. Yongsheng Wu (Bedford Institute of Oceanography, Canada) for their help in setting up the model. This research is funded by the Innovation Program of Shanghai Municipal Education Commission (2021-01-07-00-07- E00093), and the National Natural Science Foundation of China (NSFC-41976070, 41730531).

### Authors' contributions

QZ collected and analyzed the bathymetric data, modelled hydrodynamic and sediment-dynamic change, and wrote the manuscript. DF conceived the idea, designed the experiments, revised the manuscript, and acquired the funding. TF designed the model, and revised the manuscript. JT analyzed the data, and revised the manuscript. XG collected and analyzed the bathymetric data. All authors contributed to the article and approved the submitted version.

### Availability of data and materials

The dataset supporting the conclusions of this article can be found in the main text. Further inquiries can be directed to the corresponding author.

## Declarations

### Competing interests

The authors declare that the research was conducted in the absence of any commercial or financial relationships that could be construed as a potential conflict of interest.

### Author details

<sup>1</sup>State Key Laboratory of Marine Geology, Tongji University, Shanghai 200092, China. <sup>2</sup>Nanjing Hydraulic Research Institute, Nanjing 210029, China. <sup>3</sup>Shanghai Institute of Geological Survey, Shanghai 200072, China.

Received: 1 August 2022 Revised: 12 September 2022 Accepted: 18 September 2022

Published online: 27 September 2022

## References

- Anthony EJ, Brunier G, Besset M, Goichot M, Dussouillez P, Nguyen VL (2015) Linking rapid erosion of the Mekong River delta to human activities. *Sci Rep* 5(1):1–12. <https://doi.org/10.1038/srep14745>
- Chen C, Beardsley RC, Cowles G, Qi J, Lai Z, Gao G et al (2012) An unstructured-grid, finite-volume community ocean model: FVCOM user manual. Sea Grant College Program, Massachusetts Institute of Technology, Cambridge
- Chen W, Gu J, Li W, Qin X (2011) Analysis of the channel cubage of the north branch of the Yangtze River estuary with BP neural network. *Mar Sci* 35(1):70–74 (in Chinese)
- Dai Z, Du J, Chu A, Zhang X (2011) Sediment characteristics in the north branch of the Yangtze estuary based on radioisotope tracers. *Environ Earth Sci* 62(8):1629–1634. <https://doi.org/10.1007/s12665-010-0647-7>
- Dai Z, Fagherazzi S, Mei X, Chen J, Meng Y (2016) Linking the infilling of the north branch in the Changjiang (Yangtze) estuary to anthropogenic activities from 1958 to 2013. *Mar Geol* 379:1–12. <https://doi.org/10.1016/j.margeo.2016.05.006>
- Dam G, Van der Wegen M, Labeur RJ, Roelvink D (2016) Modeling centuries of estuarine morphodynamics in the Western Scheldt estuary. *Geophys Res Lett* 43(8):3839–3847. <https://doi.org/10.1002/2015GL066725>
- De Vriend HJ, Wang Z, Ysebaert T, Herman PM, Ding P (2011) Eco-morphological problems in the Yangtze estuary and the Western Scheldt. *Wetlands* 31(6):1033–1042. <https://doi.org/10.1007/s13157-011-0239-7>
- Fan D, Kuang C, Liu S, Liu A (2013) Impacts of mega-engineers in Changjiang River catchment on coastal land reclamation and wetland conservation. *J Tongji University (Natural Science)* 41(3):458–464 (in Chinese)
- Fan D, Li C, Wang D, Wang P, Archer AW, Greb SF (2004) Morphology and sedimentation on open-coast intertidal flats of the Changjiang Delta, China. *J Coastal Res SI* (43):23–35. <https://www.jstor.org/stable/25737020>
- Fan D, Wu Y, Zhang Y, Burr G, Huo M, Li J (2017) South flank of the Yangtze Delta: past, present, and future. *Mar Geol* 392:78–93. <https://doi.org/10.1016/j.margeo.2017.08.015>
- Fan D, Xu J, Wu Y, Lee G (2019) Coastal environmental changes under increasing anthropogenic impacts: an introduction. *Anthropocene Coasts* 2(1):5–12. <https://doi.org/10.1139/anc-2019-0011>
- Guo L, Xie W, Xu F, Wang X, Zhu C, Meng Y et al (2022) A historical review of sediment export–import shift in the north branch of Changjiang estuary. *Earth Surf Process Landf* 47(1):5–16. <https://doi.org/10.1002/esp.5084>
- Guo X, Fan D, Zheng S, Wang H, Zhao B, Qin C (2021) Revisited sediment budget with latest bathymetric data in the highly altered Yangtze (Changjiang) estuary. *Geomorphology* 391:107873. <https://doi.org/10.1016/j.geomorph.2021.107873>
- Han Z, Dai Z (2002) Reclamation and river training in the Qiantang estuary. In: Chen J (ed) *Engineered coasts*. Kluwer Academic Press, pp 121–138
- Jiang C, Chen S, Pan S, Fan Y, Ji H (2018) Geomorphic evolution of the Yellow River Delta: quantification of basin-scale natural and anthropogenic impacts. *Catena* 163:361–377. <https://doi.org/10.1016/j.catena.2017.12.041>
- Kuenzer C, Heimhuber V, Day J, Varis O, Bucx T, Renaud F et al (2020) Profiling resilience and adaptation in mega deltas: a comparative assessment of the Mekong, yellow, Yangtze, and Rhine deltas. *Ocean Coastal Manag* 198:105362. <https://doi.org/10.1016/j.ocecoaman.2020.105362>
- Li B (2006) Channel evolution in north branch of Changjiang River estuary since 1984. *Hydro-science and Engineering* 3:9–17 (in Chinese)
- Li M (2010) The effect of reclamation in areas between islands in a complex tidal estuary on the hydrodynamic sediment environment. *J Hydrodyn* 22(3):338–350. [https://doi.org/10.1016/S1001-6058\(09\)60063-9](https://doi.org/10.1016/S1001-6058(09)60063-9)
- Li Z, Li MZ, Dai Z, Zhao F, Li J (2015) Intratidal and neap-spring variations of suspended sediment concentrations and sediment transport processes in the north branch of the Changjiang estuary. *Acta Oceanol Sin* 34(1):137–147. <https://doi.org/10.1007/s13131-015-0605-z>
- Li Z, Wang Y, Cheng P, Zhang G, Li J (2016) Flood-ebb asymmetry in current velocity and suspended sediment transport in the Changjiang estuary. *Acta Oceanol Sin* 35(10):37–47. <https://doi.org/10.1007/s13131-016-0923-9>
- Lu Y, Liang S, Sun Z (2015) Cumulative effects of topography change on waterway's hydrodynamic along the southern coast of Hangzhou Bay. *Mar Environ Sci* 34:384–390 (in Chinese)
- Lyu H, Zhu J (2018) Impact of the bottom drag coefficient on saltwater intrusion in the extremely shallow estuary. *J Hydrol* 557:838–850. <https://doi.org/10.1016/j.jhydrol.2018.01.010>
- Ma G, Shi F, Liu S, Qi D (2013) Migration of sediment deposition due to the construction of large-scale structures in Changjiang estuary. *Appl Ocean Res* 43:148–156. <https://doi.org/10.1016/j.apor.2013.09.002>
- Mao Z, Yu Z, Xu H (2014) Study of tidal flats in Shanghai. East China Normal University Press, Shanghai
- Muller RM, Chen Y, Stefan GJ, Chan Y, Theunis P, Dirk S et al (2020) Ecological impact of land reclamation on Jiangsu coast (China): a novel ecotope assessment for Tongzhou Bay. *Water Sci Eng* 13(1):57–64. <https://doi.org/10.1016/j.wse.2020.04.001>
- Ni Y, Lin J (2003) The effects of regulation and reclamation in Qiantang estuary on Hangzhou Bay. *Ocean Eng* 21(3):73–77 (in Chinese)
- Nnafie A, Van Oyen T, De Maerschalck B, Van der Vegt M, Van der Wegen M (2018) Estuarine channel evolution in response to closure of secondary basins: an observational and morphodynamic modeling study of the Western Scheldt estuary. *J Geophys Res Earth Surface* 123(1):167–186. <https://doi.org/10.1002/2017JF004364>
- Obodoefuna DC, Fan D, Guo X, Li B (2020) Highly accelerated siltation of abandoned distributary channel in the Yangtze Delta under everchanging social-ecological dynamics. *Mar Geol* 429:106331. <https://doi.org/10.1016/j.margeo.2020.106331>
- Park JW, Park SS (1998) Hydrodynamic modeling of tidal changes due to land reclamation in an open-ended harbor, Pusan, Korea. *J Environ Sci Health Part A* 33(5):877–890. <https://doi.org/10.1080/10934529809376767>
- Qi J, Chen C, Beardsley RC, Perrie W, Cowles GW, Lai Z (2009) An unstructured-grid finite-volume surface wave model (FVCOM-SWAVE): implementation, validations and applications. *Ocean Model* 28(1–3):153–166. <https://doi.org/10.1016/j.ocemod.2009.01.007>
- Qian S, Wang D, Zhang J, Li C (2021) Adjoint estimation and interpretation of spatially varying bottom friction coefficients of the M2 tide for a tidal model in the Bohai, yellow and East China seas with multi-mission satellite observations. *Ocean Model* 161:101783. <https://doi.org/10.1016/j.ocemod.2021.101783>
- Ralston DK, Geyer WR, Lerczak JA (2010) Structure, variability, and salt flux in a strongly forced salt wedge estuary. *Journal of Geophysical Research: Oceans* 115(C6). <https://doi.org/10.1029/2009JC005806>
- Shen Y, Jia H, Li C, Tang J (2018) Numerical simulation of saltwater intrusion and storm surge effects of reclamation in Pearl River estuary, China. *Appl Ocean Res* 79:101–112. <https://doi.org/10.1016/j.apor.2018.07.013>
- Shin HJ, Lee GH, Kang K, Park Y (2019) Shift of estuarine type in altered estuaries. *Anthropocene Coasts* 2(1):145–170. <https://doi.org/10.1139/anc-2018-0013>
- Stanev EV, Dobrynin M, Pleskachevsky A, Grayek S, Günther H (2009) Bed shear stress in the southern North Sea as an important driver for suspended sediment dynamics. *Ocean Dyn* 59(2):183–194. <https://doi.org/10.1007/s10236-008-0171-4>
- Stark J, Smolders S, Vandenbruwaene W (2019) Using numerical simulations to improve insight on the historical evolution of tides and morphology in the Scheldt estuary. 38th IAHR world congress; Panama

- Swinkels CM, Jeuken CM, Wang Z, Nicholls RJ (2009) Presence of connecting channels in the Western Scheldt estuary. *J Coast Res* 25(3):627–640. <https://doi.org/10.2112/06-0719.1>
- Syvitski J, Kettner A, Correggiari A, Nelson B (2005) Distributary channels and their impact on sediment dispersal. *Mar Geol* 222:75–94. <https://doi.org/10.1016/j.margeo.2005.06.030>
- Syvitski J, Saito Y (2007) Morphodynamics of deltas under the influence of humans. *Glob Planet Chang* 57(3–4):261–282. <https://doi.org/10.1016/j.gloplacha.2006.12.001>
- Teng L, Cheng H, de Swart HE, Dong P, Li Z, Li J et al (2021) On the mechanism behind the shift of the turbidity maximum zone in response to reclamations in the Yangtze (Changjiang) estuary, China. *Marine Geology* 440:106569. <https://doi.org/10.1016/j.margeo.2021.106569>
- Tessler Z, Vörösmarty C, Grossberg M, Gladkova I, Aizenman H, Syvitski J et al (2015) Profiling risk and sustainability in coastal deltas of the world. *Science* 349(6248):638–643. <https://doi.org/10.1126/science.aab3574>
- Tian B, Wu W, Yang Z, Zhou Y (2016) Drivers, trends, and potential impacts of long-term coastal reclamation in China from 1985 to 2010. *Estuarine Coastal & Shelf Science* 170:83–90. <https://doi.org/10.1016/j.ecss.2016.01.006>
- Van den Berg JH, Jeuken CJ, Van der Spek AJ (1996) Hydraulic processes affecting the morphology and evolution of the Westerschelde estuary. In: Nordstrom KF, Roman CT (eds) *Estuarine shores—evolution, environments and human alterations*. Wiley, Chichester, pp 157–184
- Van der Spek AJ (1997) Tidal asymmetry and long-term evolution of Holocene tidal basins in the Netherlands: simulation of palaeo-tides in the Schelde estuary. *Mar Geol* 141(1–4):71–90. [https://doi.org/10.1016/S0025-3227\(97\)00064-9](https://doi.org/10.1016/S0025-3227(97)00064-9)
- Van Veen J, Van der Spek AJ, Stive MJ, Zitman T (2005) Ebb and flood channel systems in the Netherlands tidal waters. *J Coast Res* 21(6):1107–1120. <https://doi.org/10.2112/04-0394.1>
- Ve ND, Fan D, Vuong BV, Lan TD (2021) Sediment budget and morphological change in the red River Delta under increasing human interferences. *Mar Geol* 431:106379. <https://doi.org/10.1016/j.margeo.2020.106379>
- Wan Z, Ren Z, Wang X, Zheng H (2016) Application of unstructured grid finite-volume coastal ocean model (FVCOM) to the Yangtze River hypoxic zone. *Int J Numerical Methods Heat Fluid Flow* 26(8):2410–2418. <https://doi.org/10.1108/HFF-07-2015-0259>
- Wilcock PR (1996) Estimating local bed shear stress from velocity observations. *Water Resour Res* 32(11):3361–3366. <https://doi.org/10.1029/96WR02277>
- Wu C, Bao Y, Ren J, Shi H (2006a) A numerical simulation and morphodynamic analysis on the evolution of the Zhujiang River Delta in China: 6000~2500 a BP. *Acta Oceanol Sin* 28(4):64–80 (in Chinese)
- Wu F, Tong C (2017) Evolution of the north branch of Yangtze estuary in last 30 years and corresponding effects on species diversity. *Acta Oceanol Sin* 39(2):72–85 (in Chinese)
- Wu H, Zhu J, Chen B, Chen Y (2006b) Quantitative relationship of runoff and tide to saltwater spilling over from the north branch in the Changjiang estuary: a numerical study. *Estuar Coast Shelf Sci* 69(1–2):125–132. <https://doi.org/10.1016/j.ecss.2006.04.009>
- Wu J, Liu JT, Wang X (2012) Sediment trapping of turbidity maxima in the Changjiang estuary. *Mar Geol* 303:14–25. <https://doi.org/10.1016/j.margeo.2012.02.011>
- Wu Z, Saito Y, Zhao D, Zhou J, Cao Z, Li S et al (2016) Impact of human activities on subaqueous topographic change in Lingding Bay of the Pearl River estuary, China, during 1955–2013. *Sci Rep* 6(1):1–10. <https://doi.org/10.1038/srep37742>
- Xie D, Pan C, Wu X, Gao S, Wang Z (2017) Local human activities overwhelm decreased sediment supply from the Changjiang River: continued rapid accumulation in the Hangzhou Bay-Qiantang estuary system. *Mar Geol* 392:66–77. <https://doi.org/10.1016/j.margeo.2017.08.013>
- Xie D, Wang Z, Gao S, De Vriend HJ (2009) Modeling the tidal channel morphodynamics in a macro-tidal embayment, Hangzhou Bay, China. *Continent Shelf Res* 29(15):1757–1767. <https://doi.org/10.1016/j.csr.2009.03.009>
- Xie D, Wang Z, Van der Wegen M, Huang J (2021) Morphodynamic modeling the impact of large-scale embankment on the large bar in a convergent estuary. *Mar Geol* 442:106638. <https://doi.org/10.1016/j.margeo.2021.106638>
- Yang C, Gao Z, Yu Z (2016) Quantitative analysis of the characteristics of channel storage changes in the north branch of the Yangtze River estuary. *Adv Water Sci* 27(3):392–402 (in Chinese)
- Yang H, Zhang X, Cai H, Hu Q, Liu F, Yang Q (2020) Seasonal changes in river-tide dynamics in a highly human-modified estuary: Modaomen estuary case study. *Mar Geol* 427:106273. <https://doi.org/10.1016/j.margeo.2020.106273>
- Yang Z, Khangaonkar T (2009) Modeling tidal circulation and stratification in Skagit River estuary using an unstructured grid ocean model. *Ocean Model* 28(1–3):34–49. <https://doi.org/10.1016/j.ocemod.2008.07.004>
- Zhan Q, Li M, Liu X, Chen J, Chen Z (2020) Sedimentary transition of the Yangtze subaqueous delta during the past century: inspiration for delta response to future decline of sediment supply. *Mar Geol* 428:106279. <https://doi.org/10.1016/j.margeo.2020.106279>
- Zhang E, Gao S, Savenije HG, Si C, Cao S (2019a) Saline water intrusion in relation to strong winds during winter cold outbreaks: north branch of the Yangtze estuary. *J Hydrol* 574:1099–1109. <https://doi.org/10.1016/j.jhydrol.2019.04.096>
- Zhang J, Hu Z, Huang Z (2007) Analysis of the changes and formation causes of tidal bore at the north bayou of the Yangtze River estuary in recent years. *Adv Water Sci* 18(5):724–729 (in Chinese)
- Zhang W, Ruan X, Zheng J, Zhu Y, Wu H (2010) Long-term change in tidal dynamics and its cause in the Pearl River Delta, China. *Geomorphology* 120(3–4):209–223. <https://doi.org/10.1016/j.geomorph.2010.03.031>
- Zhang W, Xu Y, Hoiink AJF, Sassi MG, Zheng J, Chen X et al (2015) Morphological change in the Pearl River Delta, China. *Mar Geol* 363:202–219. <https://doi.org/10.1016/j.margeo.2015.02.012>
- Zhang Y, Zhang Z, Liu Y, Zhang H, Chen Y (2019b) Sediment dynamic processes in north branch of yangtze river estuary and response to human activities. *Yangtze River* 50(09):24–29 (in Chinese)
- Zhu Q, Yang S, Ma Y (2014) Intra-tidal sedimentary processes associated with combined wave–current action on an exposed, erosional mudflat, south-eastern Yangtze River Delta, China. *Mar Geol* 347:95–106. <https://doi.org/10.1016/j.margeo.2013.11.005>

## Publisher's Note

Springer Nature remains neutral with regard to jurisdictional claims in published maps and institutional affiliations.